ELSEVIER

Wetting behaviour of SiC ceramics
Part I. E₂O₃/Al₂O₃ additive system

F.V. Motta, R.M. Balestra, S. Ribeiro*, S.P. Taguchi

*Department of Materials Engineering (DEMAR), Faculty of Chemical Engineering of Lorena (FAENQUIL),
Polo Urbo Industrial, Gleba AI6, CP 116, 12600-000 Lorena, SP, Brazil*

Abstract

Wettability is the most important phenomenon in SiC liquid phase sintering. This paper discusses the ceramic–ceramic wetting of E_2O_3/ Al_2O_3 additives on SiC, where E_2O_3 is a mixture of rare earth oxide. A sphere-shaped sample of additive was put on a SiC plate and the set placed in a graphite resistance furnace and heated to the additive sphere melting point at a rate of 10 °C/min. The behaviour of the additive on the SiC plate was observed by means of an imaging system using a CCD camera, while the contact angle was measured and analyzed using QWin Leica software. The tests were performed in argon or nitrogen atmospheres. The wettability curves displayed a fast decline and good spreading. The E_2O_3/Al_2O_3 system, which approached a eutectic composition when compared with the phase diagram of the Y_2O_3/Al_2O_3 system, displayed better spreading. Measurements of the contact angle could not be made when the test was conducted in a nitrogen atmosphere because of the bubbles that formed in the liquid during the test, damaging the interfacial zone between E_2O_3/Al_2O_3 and SiC. The results of these tests indicate that the best sintering atmosphere for this additive system is argon.
© 2004 Elsevier B.V. All rights reserved.

Keywords: Wettability; Liquid phase sintering; Silicon carbide; Rare earth; Alumina

1. Introduction

Silicon carbide, SiC, is a well-known and important ceramic material with interesting properties such as low density, low porosity, and good wear resistance in sliding and abrasive environments, excellent corrosion resistance in chemical environments, low thermal expansion and high thermal conductivity that provide excellent thermal shock resistance [1].

High densification of SiC compacts is possible only at extremely high sintering pressures and/or temperatures exceeding 2100 °C due to the low self-diffusion coefficient. Therefore, liquid phase sintering is normally used to increase the density of SiC.

Metal oxides can be used as additives in liquid phase sintering. Negita [2] studied the probability of chemical reactions between SiC and several oxides at 2127 °C, demonstrating that the most stable of the 23 oxides investigated were Al_2O_3, BeO, HfO_2, ThO_2, Sm_2O_3, Y_2O_3, La_2O_3, Ce_2O_3. This indicates that most of the oxides that remain stable in the presence of SiC are composed of rare earth. For this reason, the additive used in this work was E_2O_3/Al_2O_3. E_2O_3 is a mixture of rare earth oxide from Xenotime, an yttrium-rich phosphate ore (E, Y)PO_4. This process is based on the alkaline fusion of the ore with NaOH, followed by aqueous and acid leaching, precipitation by oxalic acid and subsequent calcination. The final product is a solid solution of rare earth (Y^{3+}, Er^{3+}, Yb^{3+}, Dy^{3+}, Ho^{3+}). This additive system, which is relatively new in the literature, especially in SiC ceramics, has been used successfully in Si_3N_4 liquid phase sintering [3–5].

The most important phenomenon observed in liquid phase sintering is wettability. Wettability has most commonly been studied in metal–metal and metal–ceramic joining [6–8]. Wettability is based on the interfacial energies of the solid–liquid–vapour system.

Fig. 1(a) shows two independent interfaces: a solid–vapour interface (A_{SV}) and a liquid–vapour interface (A_{LV}); each surface has both γ^{SV} and γ^{LV} energies.

* Corresponding author. Tel.: +55-12-3159-9913; fax: +55-12-3153-3006.
 E-mail address: sebastiao@demar.faenquil.br (S. Ribeiro).
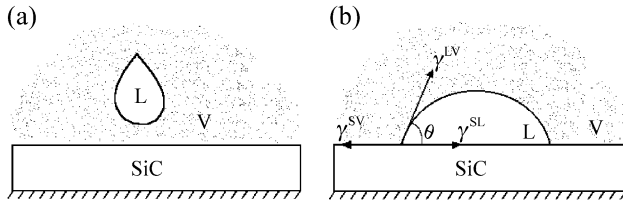
(a)   (b)

Fig. 1. Representation of wetting (a) before adhesion, and (b) after adhesion.

When a liquid drop touches the solid phase, Fig. 1(b), the individual solid and liquid areas disappear, giving place to a new solid–liquid area (A^{SL}) and the respective interfacial energy γ^{SL}. Based on Fig. 1, the system's free energy equation can be deduced mathematically.

$$G_1 = A_{LV}\gamma^{LV} + A_{SV}\gamma^{SV} \qquad (1)$$

$$G_2 = A_{SV}\gamma^{SV} + A_{LV}\gamma^{LV} + A_{SL}\gamma^{SL} \qquad (2)$$

where G_1 and G_2 are Gibbs free energies before and after wetting, respectively, as shown in Fig. 1.

Which implies that $A_{SL} = 1$, so:

$$G_2 = (A_{SV} - 1)\gamma^{SV} + (A_{LV} - 1)\gamma^{LV} + \gamma^{SL} \qquad (3)$$

Thus, the change in free energy can be calculated as:

$$\Delta G = G_2 - G_1 = (A_{SV} - 1)\gamma^{SV} + (A_{LV} - 1)\gamma^{LV}$$
$$+ \gamma^{SL} - A_{LV}\gamma^{LV} - A_{SV}\gamma^{SV} \qquad (4)$$

$$\Delta G = \gamma^{SL} - \gamma^{SV} - \gamma^{LV} \qquad (5)$$

The variables γ^{SL} and γ^{SV} are difficult to determine but, based on Fig. 1(b), ΔG can be calculated as a function of γ^{LV}. In equilibrium, Fig. 1(b) yields:

$$\gamma^{SV} = \gamma^{SL} + \gamma^{LV}\cos\theta \quad \therefore \quad \gamma^{SL} - \gamma^{SV} = -\gamma^{LV}\cos\theta \qquad (6)$$

Replacing Eq. (6) for Eq. (5):

$$\Delta G = -\gamma^{LV}(1 + \cos\theta) \qquad (7)$$

where ΔG is the Gibbs energy change in system and θ is the contact angle of systems.
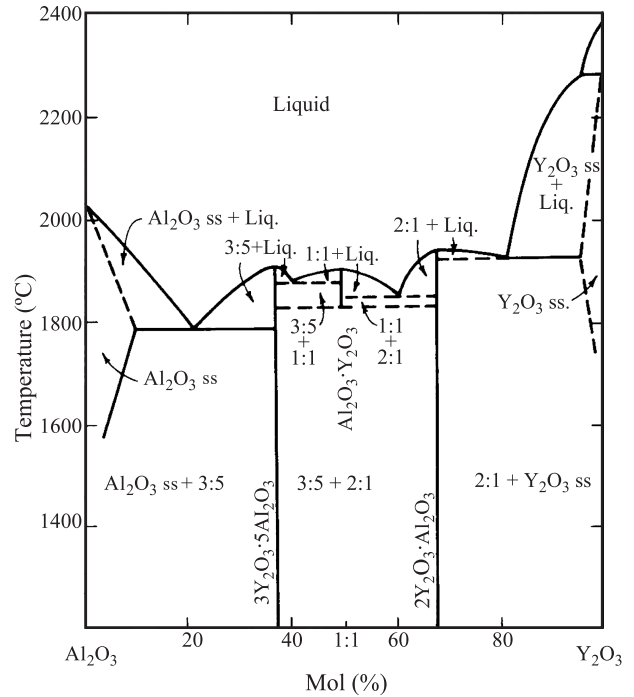

Fig. 2. Phase diagram of the Y_2O_3/Al_2O_3 system [15].

Eq. (7) shows that, when the contact angle approaches low values, ΔG decreases, thus causing the wetting to increase. The atmosphere interferes in the wettability and viscosity of liquid [9–11].

According to a review of the literature [12–14], no work has been done on the E_2O_3/Al_2O_3 system. This work presents the ceramic–ceramic wetting of this system of additives on SiC.

2. Experimental

The materials used for the wettability study were silicon carbide, SiC, plates ($10.0 \times 10.0 \times 4.0$ mm^3) having 98.9% T.D., manufactured by Wacker-Chemie, Germany. The plates were polished with 1-μm diamond paste.

The additives used were Al_2O_3 (CR6, AS 250 KC supplied by Baikalox) and the rare earth oxide E_2O_3, produced by the Department of Materials Engineering of the Faculty of Chemical Engineering of Lorena. Table 1 shows the composition of the rare earth oxides.

Table 1
Chemical composition of the E_2O_3

Oxide	wt. %	Oxide	wt. %
Y_2O_3	43.90	Sm_2O_3	0.41
Yb_2O_3	17.00	Pr_2O_3	0.27
Er_2O_3	13.60	CeO_2	0.18
Dy_2O_3	11.00	Nd_2O_3	0.18
Ho_2O_3	3.10	Eu_2O_3	0.06
Tm_2O_3	2.50	La_2O_3	0.04
Tb_2O_3	2.41	ZrO_2	1.06
Lu_2O_3	2.00	SiO_2	0.09
Gd_2O_3	1.73	Insoluble	0.56

Table 2
Compositions of the E_2O_3/Al_2O_3 system

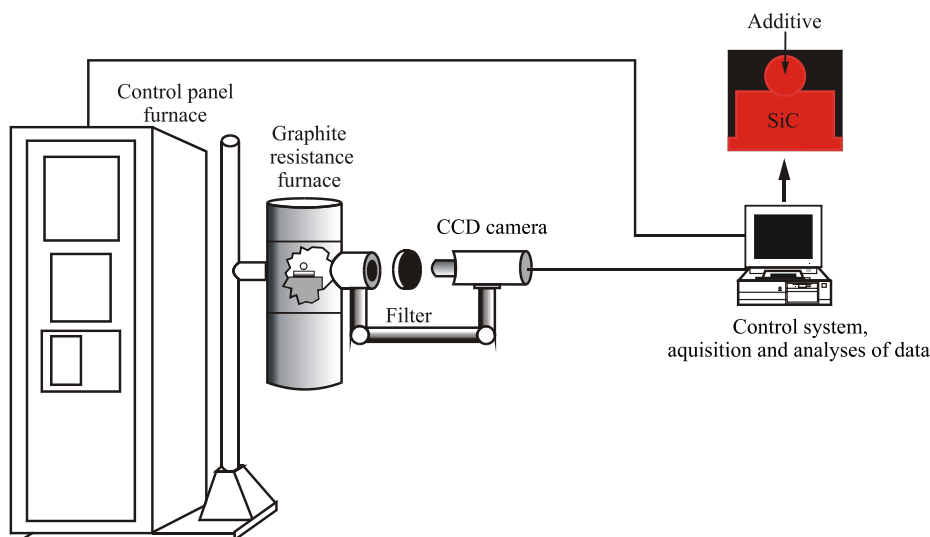| Code	E_2O_3		Al_2O_3	
	wt.%	mol%	wt.%	mol%
EA1	20.0	8.17	80.0	91.83
EA2	30.0	13.25	70.0	86.75
EA3	40.0	19.19	60.0	80.81
EA4	50.0	26.26	50.0	73.74
EA5	60.0	34.82	40.0	65.18

Fig. 3. Scheme of the wettability testing system.

Because Y_2O_3 is the major component of E_2O_3, five compositions of E_2O_3/Al_2O_3 additives were chosen, using the Y_2O_3/Al_2O_3 diagram phase for comparison (Fig. 2) [15]. One of these additives is a eutectic composition with a low melting point, while the other compositions are rich or poor in E_2O_3. Table 2 shows the additive mixtures.

The mixtures of additives were weighed on a 1×10^{-4} precision scale and mixed in isopropyl alcohol in an attrition mill for 1 h at 1000 rpm. The suspension was dried at 80 °C in a rotating drier.

The mixtures were compacted into 4.0 mm diameter spheres and pressed in a semi-isostatic press (Monostatic 50 Powder Press–Simac) at a pressure of 90 MPa.

An additive sphere was then put on the SiC plate and the set placed in a graphite resistance furnace (Astro) heated to the additive sphere melting point at a heating rate of 10 °C/min. The behaviour of the additive on the SiC plate was analyzed by means of an imaging system with a CCD camera. The wetting test ended when the contact angle remained constant, and/or the highest experimental temperature applied was 2000 °C. The tests were performed in argon or nitrogen atmospheres. Fig. 3 shows the scheme of the experiment. The contact angle was measured and analyzed using QWin Leica software. The presence of crystalline phases of melted additive was identified by X-ray diffraction analysis (XRD, Rich Seiferst & Co. Isso-Debeyeflex 1001) with Cu kα radiation. The samples were then cut transversally and their microstructure characterized by scanning electron microscopy (SEM).

3. Results and discussion

The images of the wettability tests of all the compositions were captured by a CCD camera in argon or nitrogen atmosphere. Fig. 4 represents the evolution of liquid of the EA3 composition spreading on SiC: (a–d) in argon atmosphere, and (e–h) in nitrogen atmosphere. The EA3 composition is shown here to represent all the samples because it produced the best contact angle results.

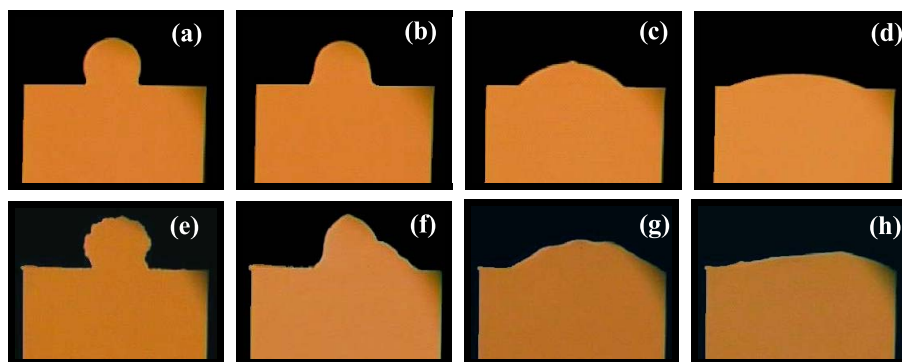It can be observed that the additive did not spread uniformly in the nitrogen atmosphere, which was attributed

Fig. 4. Sequential images of wettability tests of EA3 on SiC: in argon atmosphere at temperatures of (a) 1760 °C; (b) 1770 °C; (c) 1780 °C; and (d) 1800 °C; and in a nitrogen atmosphere at temperatures of (e) 1760 °C; (f) 1770 °C; (g) 1800 °C; and (h) 1810 °C.
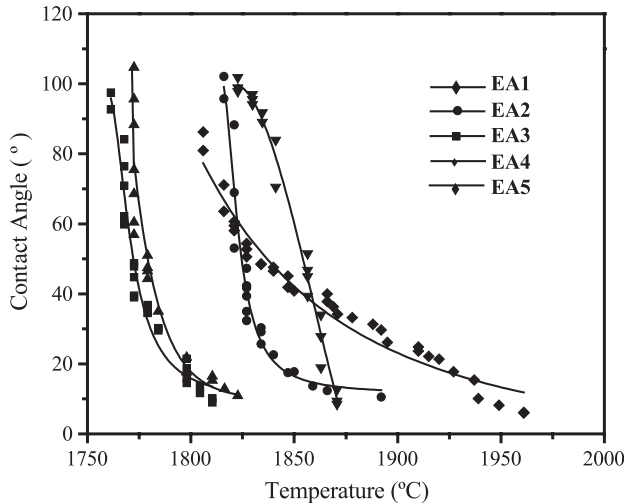
Fig. 5. Variation of contact angle with temperature.

to the formation of bubbles during the test, rendering it impossible to measure the contact angle. The formation of bubbles was caused by the nitrogen dissolved in the liquid, which increased its viscosity [1, 9–12].

The contact angle behaviour as a function of temperature of the additives on SiC is illustrated in Fig. 5. The contact angle values decreased as the temperature rose and the area of adhesion between the liquid and SiC increased.

According to Young's equation, Eq. (6), when the contact angle decreases, the γ^{LV}/γ^{SL} ratio increases. Therefore, the solid/liquid interfacial energies decrease, resulting in greater wettability. All the compositions presented θ smaller than $15°$, indicating that the E_2O_3/Al_2O_3 system has good wettability on SiC, in agreement with Eq. (7).

The EA3 composition presented a better contact angle rate than the other samples and its melting point was close to the eutectic temperature (1760 °C) of the Y_2O_3/Al_2O_3 system. Then, EA3 composition is probably similar to the eutectic composition of the Y_2O_3/Al_2O_3 system (20Y_2O_3/ 80Al_2O_3, mol%) [15]. The contact angle results obtained for the eutectic composition were the best due to the complete formation of liquid as soon as the melting point had been reached and no solid phase remained.

In cases of compositions very dissimilar from the EA3 composition, the initial spreading temperature increases, to higher percentages of E_2O_3 than of Al_2O_3.

The EA1 composition showed a smaller decrease in the contact angle rate than the other samples, i.e., the high alumina content caused slow wetting of the liquid phase on SiC.

A comparison with the Y_2O_3/Al_2O_3 phase diagram and JCDD/JCPDS files reveals that the EA3 sample was a compound of $E_3Al_5O_{12}$ and Al_2O_3 phases. Fig. 6 shows the micrograph of AE3 after the wetting test and its interface with SiC sample in argon or nitrogen atmosphere. As can be seen, the AE3 sample shows a lamellar microstructure characteristic of eutectic compositions, but is not exactly eutectic due to the appearance of primary $E_3Al_5O_{12}$ precipitate.

4. Conclusions

(a) The contact angle of E_2O_3/Al_2O_3 additive on SiC decreases with increasing temperature, improving the wetting.
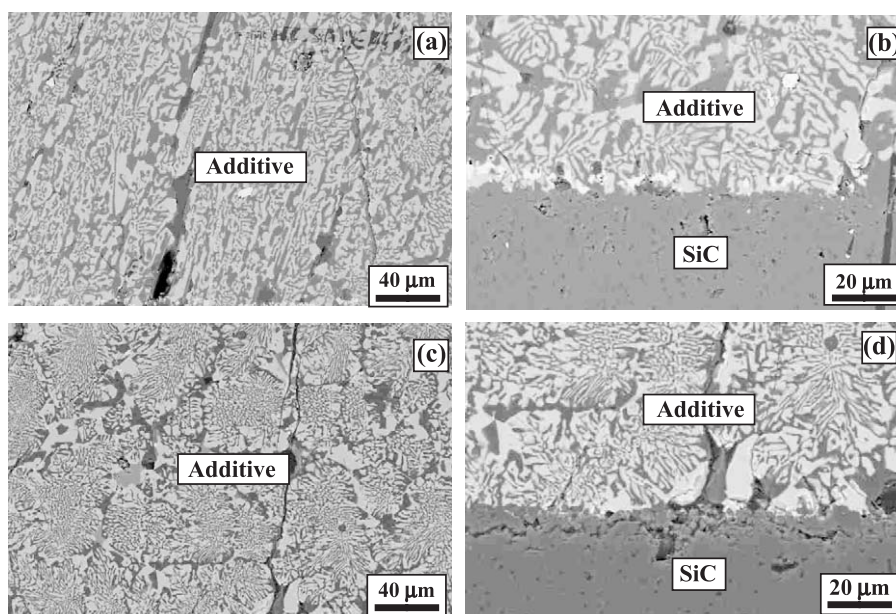

Fig. 6. EA3 micrograph of the additive after the wetting test and its interface with the SiC sample, (a–b) in argon, (c–d) and in a nitrogen atmosphere.

(b) The best spreading result in the E_2O_3/Al_2O_3 system was achieved by sample EA3, which approached a eutectic composition, as indicated by a comparison with the Y_2O_3/Al_2O_3 system.

(c) It was impossible to measure the contact angle when the test was conducted in a nitrogen atmosphere because of the formation of bubbles in the liquid during the test.

(d) The nitrogen atmosphere gave rise to a damaged zone at the E_2O_3/Al_2O_3-SiC interface. The results indicated that the best sintering atmosphere for this additive system is argon.

(e) The wettability curves displayed a sharp decline, indicating good spreading. The only exception was sample EA1, which spread more slowly than the other samples, indicating that excessive amounts of Al_2O_3 decrease the spreading velocity.

Acknowledgements

References

[1] V.A. Izhevskyi, L.A. Genova, A.H.A. Bressiani, J.C. Bressiani, Mater. Res. 3 (2000) 131.

[2] K. Negita, J. Am. Ceram. Soc. 69 (1986) 308.

[3] C. Santos, K. Strecker, S. Ribeiro, J.V.C. Souza, M.M. Silva, C.R.M. Silva, Mater. Lett. 58 (2004) 1792.

[4] K. Strecker, R. Gonzaga, S. Ribeiro, M.J. Hoffmann, Mater. Lett. 45 (2000) 39.

[5] C. Santos, S. Ribeiro, K. Strecker, C.R.M. Silva, J. Mater. Process. Technol. 142 (2003) 697.

[6] A.M. Hadian, A.L. Drew, Mater. Sci. Eng. N.A. 189 (1994) 209.

[7] P.R. Chidambaram, G.R. Edwards, D.L. Olson, Metall. Trans., B 23B (1992) 215.

[8] P. Nicolopoulos, S. Agathopolos, G.N. Angelopoulos, A. Naoumidis, H. Grubmeier, J. Mater. Sci. 27 (1992) 139.

[9] A.L. Ortiz, T. Bhatia, N.P. Padture, G.J. Pezzotti, J. Am. Ceram. Soc. 85 (2002) 1835.

[10] Y.-W. Kim, M. Mitomo, J. Am. Ceram. Soc. 82 (10) (1999) 2731.

[11] K. Biswas, G. Rixecker, I. Wiedmann, M. Schweizer, G.S. Upadhyaya, F. Aldinger, Mater. Chem. Phys. 67 (2001) 180.

[12] L. Esposito, A. Bellosi, S. Landi, J. Am. Ceram. Soc. 82 (1999) 3597.

[13] J. Chen, P. Wei, Q. Mei, Y. Huang, J. Eur. Ceram. Soc. 20 (2000) 2685.

[14] K. Landry, C. Rado, R. Voitovich, V. Eustrathopoulos, Acta Mater. 45 (1997) 3079.

[15] T. Noguchi, M. Mizuno, Kogyo Kogaku Zasshi 70 (6) (1967) 839.